

Heat-Labile Enterotoxin IIa, a Platform To Deliver Heterologous Proteins into Neurons

Chen Chen,^a Amanda Przedpelski,^a William H. Tepp,^b Sabine Pellett,^b Eric A. Johnson,^b Joseph T. Barbieri^a

Medical College of Wisconsin, Microbiology and Molecular Genetics, Milwaukee, Wisconsin, USA^a; The University of Wisconsin—Madison, Bacteriology, Madison, Wisconsin, USA^b

ABSTRACT Cholera toxin (CT) and the related heat-labile enterotoxins (LT) of *Escherichia coli* have been implicated as adjuvants in human therapies, but reactivity upon intranasal delivery dampened efforts to develop other clinical applications. However, each CT family member variant has unique biological properties that may warrant development as therapeutic platforms. In the current study, a nontoxic variant of the heat-labile enterotoxin IIa (LTIIa) was engineered to deliver heterologous, functional proteins into the cytosol of neurons. As proof of principle, the LTIIa variant delivered two cargos into neurons. LTIIa delivered β -lactamase efficiently into cells containing complex gangliosides, such as GD1b, as host receptors. LTIIa delivery of β -lactamase was sensitive to brefeldin A, an inhibitor that collapses the Golgi compartment into the endoplasmic reticulum, but not sensitive to treatment with botulinum neurotoxin D (BoNT/D), an inhibitor of synaptic vesicle cycling. LTIIa delivered a single-chain, anti-BoNT/A camelid antibody that inhibited SNAP25 cleavage during post-BoNT/A exposure of neurons. Delivery of functional, heterologous protein cargos into neurons demonstrates the potential of LTII variants as platforms to deliver therapies to inactivate toxins and microbial infections and to reverse the pathology of human neurodegenerative diseases.

IMPORTANCE This study engineered a protein platform to deliver functional, heterologous proteins into neurons. The protein platform developed was a variant of the heat-labile enterotoxin IIa (LTIIa) which lacked the catalytic domain, yielding a nontoxic protein. As proof of principle, LTIIa variants delivered two functional proteins into neurons, β -lactamase and a camelid antibody. These studies show the utility of LTIIa variants to deliver therapies into neurons, which could be extended to inactivate toxins and microbial infections and potentially to reverse the progression of neurological diseases, such as Alzheimer's disease and Parkinson's disease.

Received 30 April 2015 Accepted 21 July 2015 Published 11 August 2015

Citation Chen C, Przedpelski A, Tepp WH, Pellett S, Johnson EA, Barbieri JT. 2015. Heat-labile enterotoxin IIa, a platform to deliver heterologous proteins into neurons. *mBio* 6(4):e00734-15. doi:10.1128/mBio.00734-15.

Editor Rino Rappuoli, Novartis Vaccines and Diagnostics

Copyright © 2015 Chen et al. This is an open-access article distributed under the terms of the [Creative Commons Attribution-Noncommercial-ShareAlike 3.0 Unported license](https://creativecommons.org/licenses/by-nc-sa/4.0/), which permits unrestricted noncommercial use, distribution, and reproduction in any medium, provided the original author and source are credited.

Address correspondence to Joseph T. Barbieri, jtb01@mcw.edu.

New options have advanced medical therapies, including gene therapy, bacteriofection (bacteria as vectors for gene transfer), alternative gene therapy (AGT) (persisting bacteria produce therapeutic products *in vivo*), and protein therapeutics (1, 2). Protein therapeutics is both an early approach and an emerging field in medical therapeutics. Since the approval of insulin as a therapy (3), approximately 200 protein products that include therapeutics, diagnostics, and vaccines have been marketed (4). There are two common approaches to deliver heterologous proteins into cells, virus-based and protein-based. Protein-based therapies lack a genetic, infectious component, an advantage over virus-based therapy (5, 6). Current heterologous protein delivery platforms include protective antigen (PA) of anthrax toxin (7). PA delivery is efficient, but nonselective, since the anthrax toxin receptors are common among cell types (8), which limits PA as a cell-type-specific protein delivery platform (9). Immunotoxins (ITs) are another platform used for heterologous protein delivery (10, 11), and they are targeted by identifying receptors that have elevated expression of a host receptor on a targeted cell relative to “nontargeted” cells (12).

AB5 toxins are synthesized by several bacterial pathogens and

plants and comprise a monomeric enzymatic A subunit and a binding (B) subunit pentamer. The A subunit is a single polypeptide composed of two domains, A1 and A2, which are linked together via a disulfide bond. The A1 domain encodes a catalytic domain responsible for toxicity to the host cell. The A2 domain consists of an α -helix that penetrates into the central pore of the B subunit, thereby noncovalently anchoring the A subunit and B subunits to create the holotoxin (13). There are four main families of AB5 toxins, cholera toxin (CT), pertussis toxin, Shiga toxin, and subtilase cytotoxin, which have been previously reviewed (13). The CT family includes CT of *Vibrio cholerae* and the heat-labile enterotoxins (LTs) of *Escherichia coli*: LTI, LTIIa, LTIIb, and LTIIc (13). CT and LT enter host cells by binding gangliosides on the cell surface, leading to endocytosis and subsequent delivery of the A subunit into the host cell cytosol. CT and LT have been used as adjuvants that stimulate immunity or, alternatively, suppression of autoimmunity (14–16). However, enthusiasm for CT-based therapies waned when an adverse clinical outcome (Bell's palsy) was detected in some patients treated with intranasal LTI(K63) (17). An underappreciated property of the CT family of toxins is that individual members have unique biological properties. For

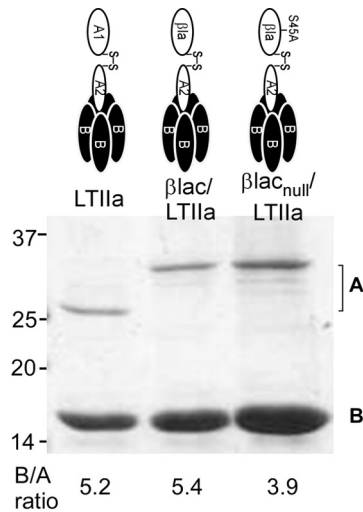


FIG 1 Primary structure of LTIIa. (Top) Schematic of LTIIa, β lac-LTIIa, and β lac_{null}-LTIIa. (Bottom) Purified LTIIa, β lac-LTIIa, and β lac_{null}-LTIIa were separated by SDS-PAGE and stained with Coomassie Blue. The ratio of B subunit to A subunit was determined by densitometry (B/A ratio is listed below each lane). Numbers at left are molecular masses in kilodaltons.

example, the LTII family members (LTIIa, LTIIb, and LTIIc) share limited primary amino acid homology or biological properties with CT and LTI (18), and Connell and coworkers showed the utility of an LTIIb variant as an adjuvant for a ricin toxin subunit vaccine (19). AB5 toxins have not been described as neuron-targeting protein delivery platforms.

Gangliosides are glycosphingolipids that contain sialic acids and are components of cell membranes. In the nervous system of higher vertebrates, complex gangliosides such as GM1a, GD1a, GD1b, and GT1b comprise about 80 to 90% of the total gangliosides (20), whereas the simple gangliosides GM2 and GM3 are more commonly displayed on extraneuronal tissue and are largely absent on brain tissue. CT and LT use gangliosides as host receptors. CT, LTI, and LTIIc bind GM1a. LTIIa binds GD1b, and LTIIb binds GD1a and other less-complex gangliosides at a lower affinity (21). Since complex gangliosides, such as GM1a, GD1a, GD1b, and GT1b, enriched neurons, LTII family members are candidates for neuron-specific protein delivery platforms.

In the current study, LTIIa is shown to deliver two functional protein cargos into the host cells, β -lactamase (β lac), which was biologically functional within the host cell cytosol, and an ~14-kDa camelid single-domain antibody that neutralized botulinum neurotoxin type A (BoNT/A) in neurons preexposed to the toxin. This shows proof of principle for the development of LTII toxin variants as protein delivery platforms for neurons.

RESULTS

β lac is catalytically active in neuronal cells. A fluorescence resonance energy transfer (FRET)-based assay (22) was used to measure β -lactamase (β lac) in the cytosol of neuronal cells. Briefly, cells were incubated with CCF2-AM, a heterocyclic small molecule, which passes across cell membranes and is converted by cytosolic host esterase to CCF2 (23), a membrane-impermeant reagent. Intracellular CCF2 has FRET properties; upon excitation at 409 nm, CCF2 transfers fluorescence resonance energy at 520 nm (green), but when cleaved by β lac, CCF2 loses FRET, which shifts

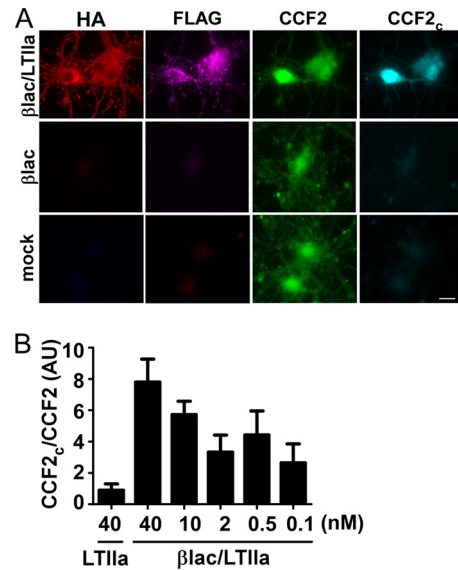


FIG 2 Dose-dependent delivery of β lac by β lac-LTIIa. (A) Rat primary cortical neurons were incubated with 40 nM β lac-LTIIa at 37°C for 60 min. Cells were incubated with CCF2-AM at RT for 30 min followed by IF to detect LTIIa bound (anti-HA, red) and β lac (anti-FLAG, magenta). Uncleaved CCF2 is shown in green, and cleaved CCF2 (CCF2_c) is shown in cyan. (B) Rat primary cortical neurons were incubated with 40 nM LTIIa or 0.1 to 40 nM β lac-LTIIa at 37°C for 60 min. Cleavage of CCF2 was quantified using the ratio of fluorescence of cleaved CCF2 to that of CCF2 as a function of added β lac-LTIIa.

emission to 447 nm (shown as cyan for visualization). Neuro-2a cells were transfected with p β lac-DsRed or p β lac_{null}-DsRed and assayed for the excitation/emission profile of CCF2. Cells expressing β lac-DsRed, but not enzymatically inactive β lac_{null}-DsRed, showed cyan fluorescence, which supported a β lac-dependent cleavage of CCF2 (see Fig. S1 in the supplemental material). This showed the CCF2- β lac reporter system to be functional in Neuro-2a cells.

β lac-LTIIa assembles into an AB5 protein. SDS-PAGE analysis assessed β lac-LTIIa assembly into an AB protein complex. Affinity-purified LTIIa, β lac-LTIIa, and β lac_{null}-LTIIa comprised two bands corresponding to the size of the A subunit or the β lac-A2 within the LTIIa chimera and B subunit, with B-A assembly ratios of 5.2 and 5.4, respectively. Since the proteins were purified with an affinity epitope located on the B subunit, the detection of the A subunits within LTIIa and β lac-LTIIa supported A-B5 assembly within β lac-LTIIa (Fig. 1).

LTIIa delivers functional cargo (β lac) into neurons. Delivery of enzymatically active β lac by β lac-LTIIa into primary rat cortical neurons was next examined. Incubation of β lac-LTIIa with rat primary cortical neurons showed CCF2 cleavage (cyan), while LTIIa did not cleave CCF2 (Fig. 2A). β lac-LTIIa titration yielded a proportional amount of CCF2 cleavage, with β lac activity detected in cells treated with 0.1 nM β lac-LTIIa (Fig. 2B). This supports the ability of LTIIa to deliver a functional, heterologous protein (β lac) into neurons.

To further investigate the trafficking of the β lac (cargo) and B subunit of β lac-LTIIa, a FLAG epitope was engineered on the C terminus of β lac to detect cargo localization, while a hemagglutinin (HA) epitope was engineered to detect the B subunit. FLAG and HA epitopes had a Pearson coefficient (PC) of 0.64 upon

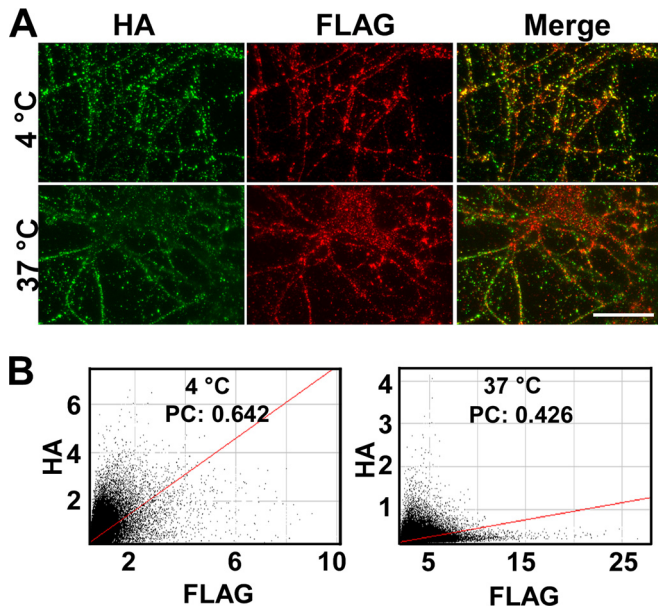


FIG 3 Delivery and separation of β lac from the B subunit during β lac-LTIIa entry into neurons. (A) Rat primary cortical neurons were incubated with 40 nM β lac-LTIIa at 4°C or 37°C for 60 min. Cells were washed, followed by IF staining, using anti-HA antibody (green) and anti-FLAG antibody (red). (B) Representative colocalization between HA and FLAG staining was shown by a cytofluorogram with Pearson's coefficient (PC) determined. Bar, 20 μ m.

incubation of β lac-LTIIa with neurons at 4°C, indicating a baseline of colocalization when bound to the cell surface (Fig. 3). Upon incubation at 37°C, the PC of FLAG/HA decreased to 0.43, showing segregation of the two epitopes. This supports neuronal cell entry and separation of cargo from the B subunit of LTIIa within neurons. In this experiment, we extrapolated that LTIIa delivered >10,000 molecules of β lac into neurons, which suggests that this LTIIa variant is efficient in delivering a heterologous cargo into a neuron.

LTIIa binds GD1b ganglioside with the highest affinity and also binds GD1a, GT1b, GQ1b, GM1a, and GD2, with lower affinities (21). Neuro-2a cells do not express complex gangliosides such as GD1b; however, upon incubation with exogenous gangliosides, Neuro-2a cell membranes can be loaded with gangliosides (24). Upon incubation of Neuro-2a cells with exogenous gangliosides, LTIIa delivered β lac ~2-fold more efficiently into GD1b-treated cells than GM1a-treated cells (Fig. 4A and B), consistent with LTIIa having a higher affinity for GD1b than GM1a (21). As a control, cells incubated with LTIIa and β lac_{null}-LTIIa did not show a translocation signal (Fig. 4A and C). Brefeldin A (BFA), a fungal metabolite that inhibits vesicular transport in the secretory pathway and vesicular exchange between endosomes and Golgi cisternae/endoplasmic reticulum (ER) in most eukaryotic cells (25), inhibited β lac translocation by LTIIa in GD1b-loaded Neuro-2a cells (Fig. 4C), supporting a Golgi compartment-mediated pathway for trafficking as native LTIIa (26). HeLa cells were also tested for β lac-LTIIa ganglioside specificity and cargo translocation efficiency. Similarly to Neuro-2a cells, GD1b-mediated entry of β lac was more efficient than GM1a-mediated entry of β lac. Neither GM2 nor GD2 mediated efficient entry of β lac (Fig. 5). Controls showed that in the absence of exogenous gangliosides, β lac delivery by β lac-LTIIa was not detected in ei-

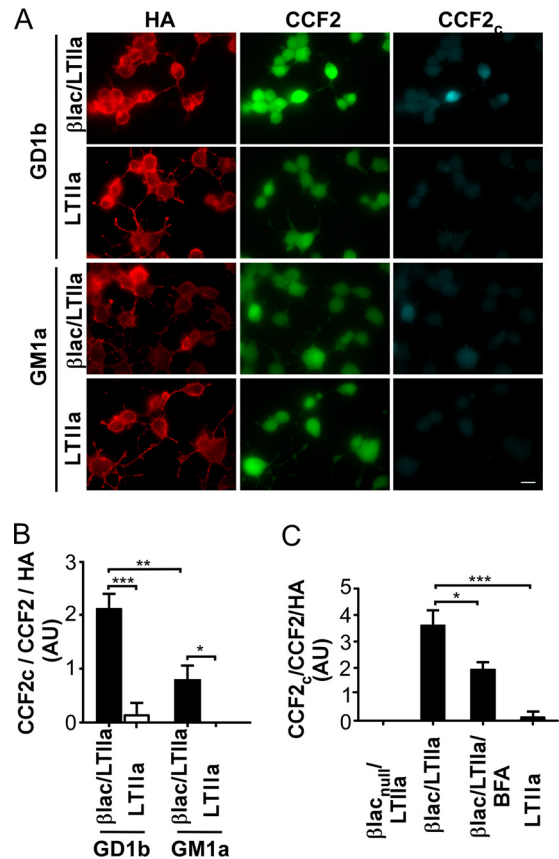


FIG 4 LTIIa delivers cargo (β lac) more efficiently into GD1b-enriched Neuro-2a cells than GM1a-enriched Neuro-2a cells. (A) Neuro-2a cells were loaded with 10 μ g/ml of ganglioside GD1b or GM1a in DMEM with 0.5% FBS at 37°C for 3 h. Cells were washed and incubated with 40 nM β lac-LTIIa or LTIIa at 37°C for 60 min. Cells were loaded with CCF2-AM at RT for 30 min, followed by IF staining using anti-HA antibody (red). Uncleaved CCF2 is shown in green, and cleaved CCF2 (CCF2_c) is shown in cyan. (B) Cleavage of substrate CCF2 was quantified using the CCF2_c/CCF2/HA ratio of fluorescent intensities. (C) Neuro-2a cells were loaded with GD1b and then incubated with 40 nM β lac-LTIIa, β lac_{null}-LTIIa, or LTIIa at 37°C for 60 min alone or with 0.1 μ g/ml of brefeldin A (BFA). Cells were washed and were loaded with CCF2-AM at RT for 30 min. Cleavage of CCF2 was quantified using the CCF2_c/CCF2/HA ratio of fluorescent intensities. Data were analyzed by two-tailed Student's *t* test. *, *P* < 0.05; **, *P* < 0.005; ***, *P* < 0.001. Bar, 20 μ m.

ther Neuro-2a or HeLa cells, as shown by the dashed line in Fig. 5. β lac-LTIIa delivered β lac more efficiently in neurons than in either Neuro-2a cells or HeLa cells. This suggests that neurons are a preferred target of β lac-LTIIa (Fig. 5).

LTIIa delivers functional cargo (β lac) into BoNT/D-intoxicated neurons. Botulinum neurotoxins cleave neuronal SNARE proteins to prevent synaptic vesicle fusion to the cell membrane. To determine if LTIIa can deliver cargo into neurons that do not cycle synaptic vesicles, the ability of β lac-LTIIa to deliver β lac into BoNT/D-intoxicated neurons was measured. Rat primary neurons were incubated overnight with BoNT/D to cleave endogenous VAMP2, which was confirmed by immunofluorescence (IF) staining (Fig. 6A and B). CCF2 cleavage by β lac-LTIIa was similar in BoNT/D-treated neurons and control neurons (Fig. 6C). Translocation of β lac by β lac-LTIIa was sensitive to BFA in BoNT-intoxicated neurons (Fig. 6C), supporting a Golgi compartment-mediated pathway for β lac trafficking. LTIIa

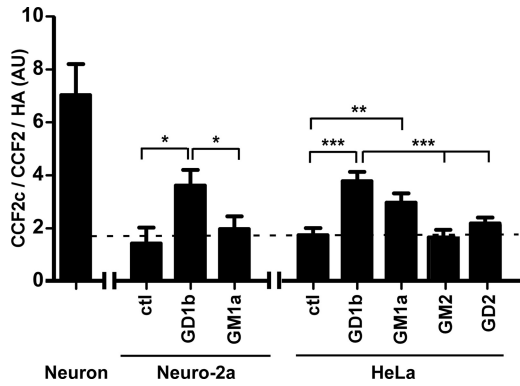


FIG 5 LTIIa delivers β lac more efficiently to neurons than to Neuro-2a cells and HeLa cells. A 40 nM concentration of β lac-LTIIa was incubated with rat cortical neurons; Neuro-2a cells loaded with GD1b or GM1a; and HeLa cells loaded with GD1b, GM1a, GM2, or GD2 at 37°C for 60 min. Cells were loaded with CCF2-AM at RT for 30 min followed by IF staining using anti-HA antibody (red). Cleavage of substrate CCF2 was quantified using the CCF2_c/CCF2/HA ratio of fluorescent intensities. The dashed line was drawn based on detectable translocation by IF. Data were analyzed by two-tailed Student's *t* test. *, $P < 0.05$; **, $P < 0.005$; ***, $P < 0.001$.

was next tested for the ability to deliver a BoNT therapeutic into neurons.

VHH-B8-LTIIa inhibits BoNT/A cleavage of SNAP25 in primary cortical neurons. An LTIIa variant was engineered where the A1 subunit was exchanged with a single-chain variable-region camelid antibody known to inhibit BoNT/A-LC (B8) (termed VHH-B8-LTIIa; GenBank accession number FJ643070) (27) (Fig. 7A). Primary cortical neurons were incubated with BoNT/A or BoNT/D for 2 h at 37°C, washed, and then incubated with various amounts of VHH-LTIIa for 3 h and assayed for cleaved SNAP25 (BoNT/A-treated cells) or degradation of full-length VAMP2 (BoNT/D-treated cells). Cleaved SNAP25 was detected in cells treated with BoNT/A alone, while BoNT/A-intoxicated cells treated with VHH-LTIIa showed a dose-dependent reduction of cleaved SNAP25 (Fig. 7B and D). Controls showed that VHH-LTIIa inhibition was BoNT serotype dependent, since VHH-LTIIa did not inhibit the cleavage of VAMP2 by BoNT/D (Fig. 7C and D). Similar results were observed when VHH-LTIIa was incubated with postintoxicated neurons overnight (Fig. 7E). Western blotting (WB), using an antibody that recognizes full-length and cleaved forms of SNAP25, showed that VHH-LTIIa partially inhibited BoNT/A cleavage of SNAP25, while VHH-LTIIa did not affect BoNT/D VAMP2 cleavage with overnight incubation in neurons (Fig. 8). This is the first example of the active delivery of a functional therapy into a BoNT-intoxicated neuron by AB5 toxin.

DISCUSSION

In this study, LTIIa was shown to deliver functional, heterologous proteins into neurons: β lac, as a reporter cargo, and a single-chain camelid antibody, as a BoNT therapy. β lac-LTIIa did not show “off-target” delivery of heterologous cargo into either Neuro-2a cells or HeLa cells, since β lac intracellular delivery into these cells required addition of exogenous gangliosides. β lac-LTIIa delivery was independent of synaptic vesicle cycling, consistent with LTIIa not entering synaptic vesicles. Overall, LTIIa appears to be a candidate platform to deliver heterologous proteins into neurons.

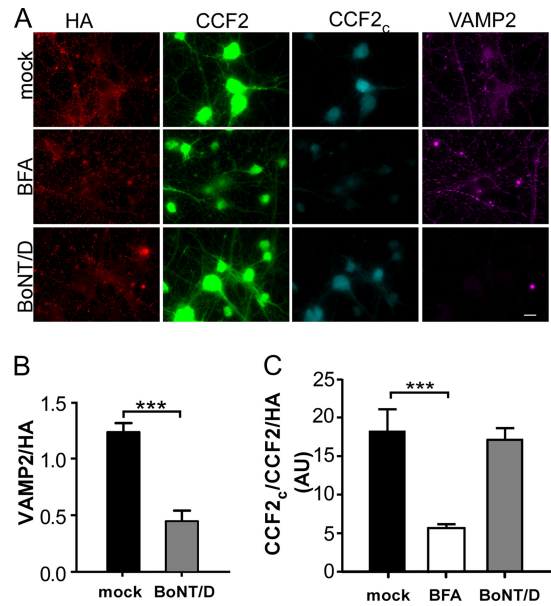


FIG 6 β lac-LTIIa cleaves CCF2 in BoNT-intoxicated primary cortical neurons. (A) Rat cortical primary neurons were incubated with 2 nM BoNT/D at 37°C for 16 h. BoNT-treated neurons were incubated with 40 nM β lac-LTIIa at 37°C for 60 min alone or with 0.1 μ g/ml brefeldin A (BFA), washed, and loaded with CCF2-AM at RT for 30 min followed by IF staining, using anti-HA antibody (red) and anti-VAMP2 (magenta), which recognizes only full-length VAMP2. Uncleaved CCF2 is shown in green, and cleaved CCF2 (CCF2_c) is shown in cyan. (B) Cleavage of VAMP2 was quantified using the VAMP2/HA ratio of fluorescent intensities. (C) Cleavage of substrate CCF2 was quantified using the CCF2_c/CCF2/HA ratio of fluorescent intensities. Data were analyzed by two-tailed Student's *t* test. ***, $P < 0.001$. Bar, 20 μ m.

The intrinsic affinity of LTIIa for the complex ganglioside GD1b provides a delivery platform that is trophic for neurological tissue. β lac translocation was more efficient in neurons than in Neuro-2a and HeLa cells, suggesting that neurons are a preferred target of β lac-LTIIa (Fig. 5). Since GM1a mediated β lac translocation in Neuro-2a and HeLa cells, further studies need to modify LTIIa B subunit to enhance GD1b binding and decrease GM1a binding to make a more neuron-specific platform. The pentameric B subunits of LTIIb were reported to activate the Toll-like receptor 2 (TLR2)/TLR1 heterodimer when not associated with the A subunit (28). Four mutated pentameric B subunits, M69E, A70D, L73E, and S74D, were defective in TLR1/2 activation despite retaining full ganglioside-binding capacity (28). Those four residues are conserved between LTIIa and LTIIb (29). Corresponding modifications of LTIIa B subunits are planned to eliminate TLR interaction to reduce immune activity of the B subunit.

BoNTs, which are tier 1, category A select agents, deliver a light-chain protease to neurons, causing cleavage of one or more SNARE proteins involved in neurotransmission, which can extend flaccid paralysis for up to 6 months (30). The primary treatment of botulism is with an antitoxin (human botulinum immunoglobulin) and supportive care. While there are no approved BoNT therapies to clear intracellular BoNT in neurons, progress has been made toward BoNT therapies, including neutralizing antibodies and BoNT heavy-chain-based drug delivery systems (31–34). Delivery systems based on BoNT/A heavy chain (33, 34) and inactivated BoNT/B-coupled liposome (35) depend on synaptic vesicle recycling, as synaptic vesicle proteins SV2 and synap-

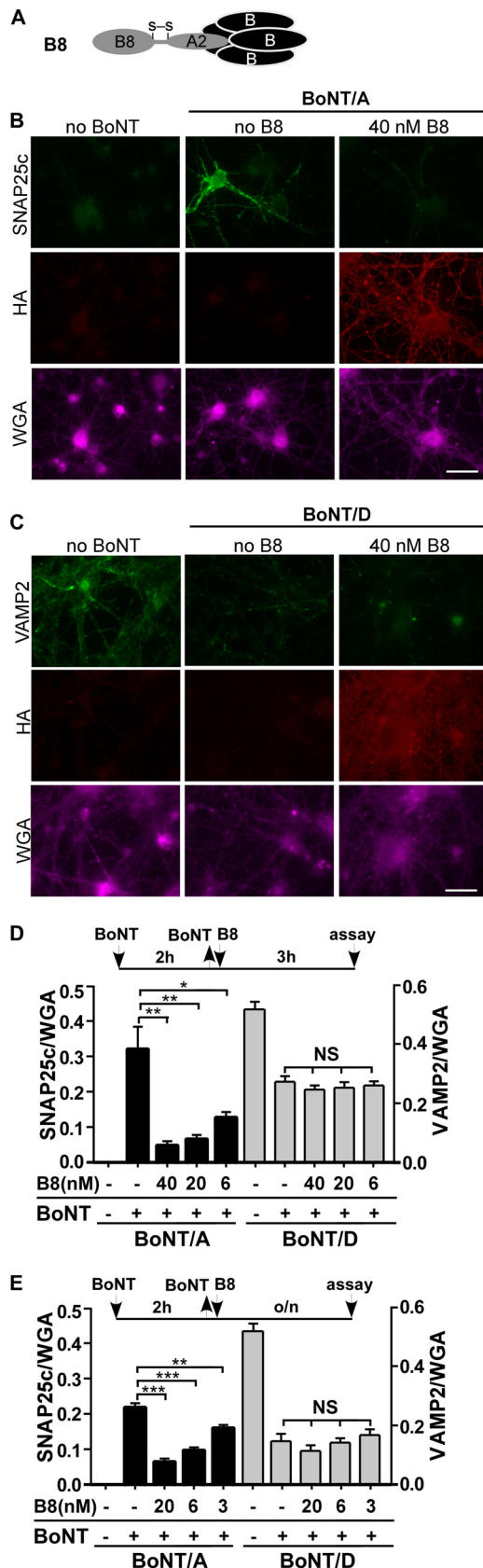


FIG 7 VHH-B8-LTIIa protects neurons from BoNT/A intoxication. (A) Schematic of VHH-B8-LTIIa. (B and C) A 1 nM concentration of BoNT/A (B) (Continued)

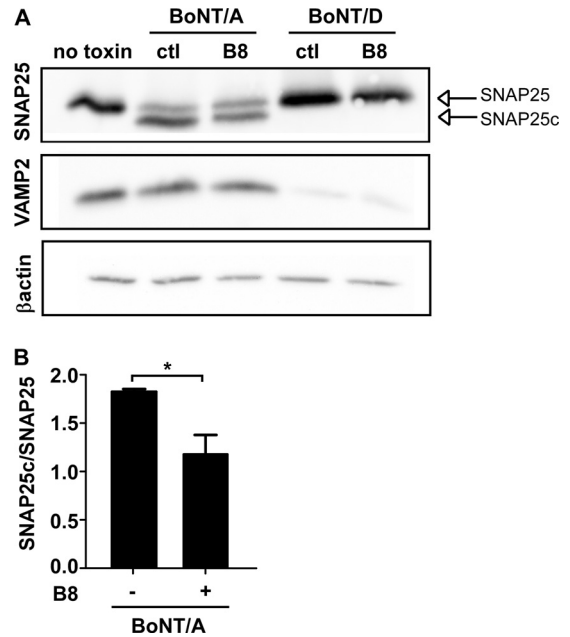


FIG 8 VHH-B8-LTIIa protects neurons from BoNT/A but not BoNT/B intoxication. (A) BoNT/A or BoNT/D (0.5 nM) with or without 20 nM VHH-B8-LTIIa (B8) was incubated with rat cortical neurons at 37°C for 24 h, when neurons were washed with PBS, lysed with radioimmunoprecipitation assay buffer, and separated by SDS-PAGE. WB was performed using anti-SNAP25 antibody (recognizing full-length and cleaved SNAP25) and VAMP2 (recognizing only full-length VAMP2) and β -actin (loading control [ctl]). (B) SNAP25 cleavage was quantified by measuring the SNAP25c/SNAP25 density ratios from three independent experiments. Data were analyzed by two-tailed Student's *t* test. *, *P* < 0.05.

totagmin II are the protein receptors for BoNT/A and BoNT/B, respectively (36–38). However, BoNT-based delivery systems are inefficient for entry into BoNT-intoxicated neurons. In contrast, BoNT/D intoxication did not affect β lac-LTIIa entry into neurons (Fig. 6). The current study shows that LTIIa could deliver a therapeutic camelid antibody (VHH) into BoNT/A-intoxicated neurons that partially inhibited BoNT/A action (Fig. 7 and 8), supporting the development of LTIIa to deliver therapeutics following BoNT intoxication. Thus, attention now focuses on engineering BoNT therapies that have a catalytic component for BoNT neutralization, such as the fusion of VHH-B8-D5 fusion proteins (39) to accelerate turnover of VHH-bound BoNT/A light chain, and the addition of an F-box domain region of TrCP (trans-

Figure Legend Continued

or BoNT/D (C) was incubated with rat cortical neurons at 37°C for 2 h, when toxin was removed and the indicated amount of VHH-B8-LTIIa (B8) was added to neurons for an additional 3 h. Cells were fixed and incubated with Alexa 647-wheat germ agglutinin (WGA; magenta) for 30 min as a cell marker. The IF assay stained for HA (red) and cleaved SNAP25 (SNAP25c, green) in BoNT/A-treated cells or intact VAMP2 (green) in BoNT/D-treated cells. (D) Cleavage was quantified by measuring the SNAP25c/WGA ratio of fluorescence intensities for BoNT/A-treated cells and the VAMP2/WGA ratio of fluorescence intensities for BoNT/D-treated cells. (E) BoNT/A or BoNT/D (1 nM) was incubated with rat cortical neurons at 37°C for 2 h, when toxin was removed and the indicated amount of VHH-B8-LTIIa (B8) was added with neurons overnight. Cleavage was quantified as described for panel D. Data were analyzed as SEM by two-tailed Student's *t* test. *, *P* < 0.05; **, *P* < 0.005. Bar, 20 μ m. NS, not significant; o/n, overnight.

ducin repeats-containing protein) (D5), an E3 ubiquitin ligase receptor, has been used to accelerate turnover of the targeted BoNT/A protease (31, 39). An adenovirus-based delivery system for VHH-based therapies has been recently described (40).

Protein aggregation in the brain is a characteristic feature of neurodegenerative disorders such as Alzheimer's disease, Parkinson's disease, amyotrophic lateral sclerosis, and Huntington's disease (41), where a therapeutic protein could be delivered to affected neurons. AB5 variants could also target latent viruses inside neurons, such as herpes zoster virus, which causes disease in 4 of every 1,000 healthy individuals each year, and a reported 10 cases per 1,000 individuals older than 75 years (42). In addition, LTIIa variants may also deliver therapeutics, either protein or non-protein based, to treat latent microbial infections in neurons.

MATERIALS AND METHODS

Antibodies. Antibodies were purchased from the vendors indicated: rat anti-HA antibody (Roche), mouse anti-FLAG M2 antibody (Sigma), mouse anti-VAMP2 (clone 69.1; SYSY), mouse anti-BoNT/A-cleaved SNAP25 (SNAP25c; 4F3-2C Research and Diagnostic Antibodies; recognizing only BoNT/A-cleaved SNAP25 but not full-length SNAP25), mouse anti-SNAP25 (SMI-81R; Covance; recognizing both full-length and BoNT-cleaved SNAP25), Alexa Fluor-labeled secondary antibodies (Invitrogen), and Alexa 647-wheat germ agglutinin (WGA) (Invitrogen).

Plasmid construction. *E. coli* codon-optimized sequences of LTIIa (GenBank accession number JQ031711) A subunit and B subunit were synthesized with dual isopropyl- β -D-thiogalactopyranoside (IPTG)-inducible T7 promoters (GenScript) and subcloned into the pET28a vector for expression. His6 and HA2 epitopes were added to the C terminus of the B subunit for purification and immunofluorescence detection, respectively. LTIIa A subunit and B subunit genes encode leader sequences for cotranslational secretion into the periplasm. TEM-1 β -lactamase (β lac; GenBank sequence accession number AGW45163.1; amino acids 24 to 286) replaced the A1 subunit of LTIIa (amino acids 1 to 172), producing β lac-LTIIa (Fig. 1), which included 3 \times FLAG downstream of the β lac. Site-directed mutagenesis (S45A) produced β lac_{null}-LTIIa, which lacked β lac activity. DNAs encoding β lac and β lac_{null} were also subcloned into DsRedmonO1 to construct p β lac-DsRed and p β lac_{null}-DsRed, respectively. DNA encoding a single-domain 14-kDa camelid antibody (VHH) specific for BoNT/A (ALc-B8; GenBank accession number FJ643070; amino acids 7 to 121) with a C-terminal 3 \times FLAG tag replaced the sequence encoding the A1 subunit of LTIIa (amino acids 1 to 172), yielding VHH-B8-LTIIa. Constructs were confirmed by DNA sequencing.

Protein expression and purification. Plasmids encoding LTIIa, β lac-LTIIa, β lac_{null}-LTIIa, and VHH-B8-LTIIa were transformed into *E. coli* BL21(DE3). Transformants were grown overnight on LB agar plates containing 50 μ g of kanamycin/ml, which were the inoculums for liquid cultures (LB, 400 ml) containing the same antibiotic. Cells were cultured at 37°C to an optical density at 600 nm (OD₆₀₀) of 0.6 when T7 promoter expression was induced with 1 mM IPTG. Cells were cultured overnight at 250 rpm at 16°C. Cells were pelleted and suspended in 20 mM Tris (pH 7.9) with 25% sucrose. Cells were treated with lysozyme (0.16 mg/ml in 0.1 M EDTA) for 30 min on ice, followed by addition of 70 mM MgCl₂ (final concentration) and centrifugation at 5,000 \times g for 20 min to separate the soluble periplasm from the cells. His6-tagged proteins were purified from the periplasm, using Ni²⁺-nitrilotriacetic acid (NTA) resin (Qiagen). Purified proteins were dialyzed into 20 mM Tris buffer (pH 7.9) with 20 mM NaCl and 40% glycerol. Aliquots were stored at -80°C.

Cells and reagents. Neuro-2a cells (ATCC; CCL-131) and HeLa cells (ATCC; CCL-2) were cultured in Dulbecco's modified Eagle's medium (DMEM; Invitrogen) with 10% fetal bovine serum (FBS; Invitrogen). Cells were transformed with p β lac-DsRed or p β lac_{null}-DsRed with Lipofectamine LTX (Invitrogen) as suggested by the manufacturer. Rat primary cortical neurons were cultured in glass-bottomed 24-well plates

(MatTek) at ~20,000 neurons/well as previously described (43). Briefly, rat E18 cortical neurons or rat E18 hippocampal neurons (BrainBits LLC) were cultured in neurobasal medium (catalog no. 21103; Invitrogen) supplemented with 0.5 mM GlutaMAX-I (catalog no. 35050; Invitrogen), 2% B27 supplement (catalog no. 17504; Invitrogen), and Primocin (InvivoGen). Half of the medium was replenished every 5th day. Neurons were used at day 10 to 14 postplating. Botulinum neurotoxin type D (BoNT/D) was isolated from *Clostridium botulinum* strain 1873. The 150-kDa protein was purified using methods similar to those previously described for isolation of toxins from other BoNT serotypes (44, 45). Specific activity in mice was 1.1 \times 10⁸ 50% lethal dose (LD₅₀) units/mg.

(i) β lac-LTIIa and LTIIa entry and translocation in Neuro-2a cells and primary cortical neurons. Neuro-2a cells and HeLa cells were loaded with 10 μ g/ml of the ganglioside GD1b, GM1a, GD2, or GM2 in DMEM with 0.5% fetal bovine serum (FBS) at 37°C for 3 h. Cells were washed and incubated with 40 nM β lac-LTIIa or LTIIa in serum-free DMEM at 37°C for 60 min. Primary neurons were incubated with 40 nM LTIIa or β lac-LTIIa in neurobasal medium (supplemented with B27 and GlutaMAX) at 37°C or 4°C for 60 min. Cells were washed with Hanks' balanced salt solution (HBSS) and loaded with CCF2-AM dye (Invitrogen; 6 \times prepared as suggested by the manufacturer to obtain a final concentration of 1 \times in HBSS). Samples were incubated at room temperature (RT) for 30 min and washed, and IF staining was performed as described below.

(ii) Effects of VHH-B8-LTIIa on BoNT-intoxicated neurons. Rat cortical neurons were incubated with 1 nM BoNT/A or BoNT/D at 37°C for 2 h, toxin was removed, and indicated amounts of VHH-B8-LTIIa (B8) were incubated with neurons at 37°C for another 3 h. Cells were fixed and incubated with Alexa 647-wheat germ agglutinin for 30 min at room temperature (RT). Immunofluorescence (IF) staining, as described below, detected BoNT/A-cleaved SNAP25 (SNAP25c) or intact VAMP2 in BoNT/D-treated cells. Cleavage of SNARE substrates was quantified using the SNAP25c/WGA ratio of fluorescence intensities for BoNT/A-intoxicated cells and the VAMP2/WGA ratio for BoNT/D-intoxicated cells. In other parameters of this experiment, neurons were incubated with 1 nM BoNT/A or BoNT/D with the indicated amounts of VHH-B8-LTIIa at 37°C overnight, and SNARE substrate cleavage was evaluated as described above. Neurons were also incubated with 0.5 nM BoNT/A and BoNT/D with 20 nM VHH-B8-LTIIa at 37°C overnight, and SNARE substrate cleavage was evaluated by Western blotting (WB) using anti-SNAP25 antibody (recognizing both full-length and cleaved forms of SNAP25) and anti-VAMP2 antibody (recognizing full-length VAMP2).

IF staining. Cells were fixed with 4% (wt/vol) paraformaldehyde in Dulbecco's phosphate-buffered saline (DPBS) for 15 min at RT, washed twice with DPBS, permeabilized with 0.1% Triton X-100 in 4% formaldehyde in DPBS for 15 min at RT, incubated with 150 mM glycine in DPBS for 10 min at RT, washed with DPBS twice, and subjected to immunofluorescence (IF) staining. Treated cells were incubated in blocking solution (10% normal goat serum, 2.5% cold fish skin gelatin [Sigma], 0.1% Triton X-100, 0.05% Tween 20 in DPBS) for 1 h (RT), followed with primary antibodies in antibody incubation solution (5% normal goat serum, 1% cold fish skin gelatin, 0.1% Triton X-100, 0.05% Tween 20 in DPBS) overnight at 4°C. Cells were washed three times with DPBS plus 0.05% Tween 20 and incubated with goat or rat IgG Alexa-labeled secondary antibodies (Invitrogen) in antibody incubation solution for 1 h (RT). Then, cells were washed 3 times, fixed with 4% paraformaldehyde in DPBS for 15 min (RT), and washed (DPBS). Mounting reagent CitiFluor AF-3 (Electron Microscopy Sciences) was added, and images were captured with a Nikon TE2000 microscope using a Photometrics CoolSnap HQ2 camera. Images were captured by epifluorescence with a Sedat Quad cube (Chroma Technology Corp.). Cleaved CCF2 (CCF2_c, shown as cyan in this paper for better visualization) was observed in the 4',6-diamidino-2-phenylindole (DAPI) channel (AT350/50x, ET455/50m). Uncleaved CCF2 (shown as green) and Alexa 488 secondary antibody-labeled staining were observed in the fluorescein isothiocyanate (FITC) channel (ET490/20x, ET525/36m). Alexa 647-WGA was observed in the Cy5

channel (ET645/30x, ET705/72m). Alexa 568 secondary antibody-labeled staining was observed in the DsRed channel (ET555/25x, ET605/52m). For the colocalization experiment, images were acquired by a total internal reflection fluorescence (TIRF) microscope equipped with a CFI Plan Apo VC 100× oil (numerical aperture [NA], 1.49) type objective.

Data analysis and statistics. Images were generated with equal exposure times and conditions. Image intensity analysis and colocalization analysis were performed using Nikon NIS-Elements and ImageJ 1.48b (NIH). Figures were compiled using Canvas X (ACD Systems). Data were shown as means with standard errors of the means (SEM). Data were analyzed by two-tailed Student's *t* test using GraphPad Prism 5.0 (GraphPad Software, CA). *P* values of <0.05 at the 95% confidence level are indicated by *, *P* values of <0.005 are indicated by **, and *P* values of <0.001 are indicated by ***.

SUPPLEMENTAL MATERIAL

Supplemental material for this article may be found at <http://mbio.asm.org/lookup/suppl/doi:10.1128/mBio.00734-15/-DCSupplemental>.

Figure S1, TIF file, 2.7 MB.

ACKNOWLEDGMENTS

Grants from NIH-NIAID AI-101313 and AI-030162 supported these studies.

We thank Madison Zuverink for providing recombinant β -lactamase in this study.

REFERENCES

- Pálffy R, Gardlík R, Hodosy J, Behuliak M, Resko P, Radványi J, Celec P. 2006. Bacteria in gene therapy: bactofection versus alternative gene therapy. *Gene Ther* 13:101–105. <http://dx.doi.org/10.1038/sj.gt.3302635>.
- Gardlík R, Pálffy R, Hodosy J, Lukács J, Turna J, Celec P. 2005. Vectors and delivery systems in gene therapy. *Med Sci Monit* 11:RA110–RA121.
- Goeddel DV, Kleid DG, Bolivar F, Heyneker HL, Yansura DG, Crea R, Hirose T, Kraszewski A, Itakura K, Riggs AD. 1979. Expression in *Escherichia coli* of chemically synthesized genes for human insulin. *Proc Natl Acad Sci U S A* 76:106–110. <http://dx.doi.org/10.1073/pnas.76.1.106>.
- Walsh G. 2010. Biopharmaceutical benchmarks 2010. *Nat Biotechnol* 28:917–924. <http://dx.doi.org/10.1038/nbt0910-917>.
- Heilmann C, von Samson P, Schlegel K, Attmann T, von Specht BU, Beyersdorf F, Lutter G. 2002. Comparison of protein with DNA therapy for chronic myocardial ischemia using fibroblast growth factor-2. *Eur J Cardiothorac Surg* 22:957–964. [http://dx.doi.org/10.1016/S1010-7940\(02\)00577-8](http://dx.doi.org/10.1016/S1010-7940(02)00577-8).
- Cui M, Wan Y, Anderson DG, Shen FH, Leo BM, Laurencin CT, Balian G, Li X. 2008. Mouse growth and differentiation factor-5 protein and DNA therapy potentiates intervertebral disc cell aggregation and chondrogenic gene expression. *Spine J* 8:287–295. <http://dx.doi.org/10.1016/j.spinee.2007.05.012>.
- Akamatsu Y, Murphy JC, Nolan KF, Thomas P, Kreitman RJ, Leung SO, Junghans RP. 1998. A single-chain immunotoxin against carcinoembryonic antigen that suppresses growth of colorectal carcinoma cells. *Clin Cancer Res* 4:2825–2832.
- Bradley KA, Mogridge J, Mourez M, Collier RJ, Young JA. 2001. Identification of the cellular receptor for anthrax toxin. *Nature* 414:225–229. <http://dx.doi.org/10.1038/n35101999>.
- Varughese M, Chi A, Teixeira AV, Nicholls PJ, Keith JM, Leppla SH. 1998. Internalization of a *Bacillus anthracis* protective antigen-c-Myc fusion protein mediated by cell surface anti-c-Myc antibodies. *Mol Med* 4:87–95.
- Trinh KR, Vasuthasawat A, Steward KK, Yamada RE, Timmerman JM, Morrison SL. 2013. Anti-CD20-interferon-beta fusion protein therapy of murine B-cell lymphomas. *J Immunother* 36:305–318. <http://dx.doi.org/10.1097/CJI.0b013e3182993eb9>.
- Olafsen T, Elgqvist J, Wu AM. 2011. Protein targeting constructs in alpha therapy. *Curr Radiopharm* 4:197–213. <http://dx.doi.org/10.2174/1874471011104030197>.
- Pastan I, Hassan R, Fitzgerald DJ, Kreitman RJ. 2006. Immunotoxin therapy of cancer. *Nat Rev Cancer* 6:559–565. <http://dx.doi.org/10.1038/nrc1891>.
- Beddoe T, Paton AW, Le Nours J, Rossjohn J, Paton JC. 2010. Structure, biological functions and applications of the AB5 toxins. *Trends Biochem Sci* 35:411–418. <http://dx.doi.org/10.1016/j.tibs.2010.02.003>.
- Sanchez J, Holmgren J. 2011. Cholera toxin—a foe and a friend. *Indian J Med Res* 133:153–163.
- McKenzie SJ, Halsey JF. 1984. Cholera toxin B subunit as a carrier protein to stimulate a mucosal immune response. *J Immunol* 133:1818–1824.
- Bharati K, Ganguly NK. 2011. Cholera toxin: a paradigm of a multifunctional protein. *Indian J Med Res* 133:179–187.
- Lewis DJ, Huo Z, Barnett S, Kromann I, Giemza R, Galiza E, Woodrow M, Thierry-Carstensen B, Andersen P, Novicki D, Del Giudice G, Rappuoli R. 2009. Transient facial nerve paralysis (Bell's palsy) following intranasal delivery of a genetically detoxified mutant of *Escherichia coli* heat labile toxin. *PLoS One* 4:e6999. <http://dx.doi.org/10.1371/journal.pone.0006999>.
- Hajishengallis G, Connell TD. 2013. Type II heat-labile enterotoxins: structure, function, and immunomodulatory properties. *Vet Immunol Immunopathol* 152:68–77. <http://dx.doi.org/10.1016/j.vetimm.2012.09.034>.
- Greene CJ, Chadwick CM, Mandell LM, Hu JC, O'Hara JM, Brey RN, Mantis NJ, Connell TD. 2013. LT-IIb(T131), a non-toxic type II heat-labile enterotoxin, augments the capacity of a ricin toxin subunit vaccine to evoke neutralizing antibodies and protective immunity. *PLoS One* 8:e69678. <http://dx.doi.org/10.1371/journal.pone.0069678>.
- Schwarz A, Futerman AH. 1996. The localization of gangliosides in neurons of the central nervous system: the use of anti-ganglioside antibodies. *Biochim Biophys Acta* 1286:247–267. [http://dx.doi.org/10.1016/S0304-4157\(96\)00011-1](http://dx.doi.org/10.1016/S0304-4157(96)00011-1).
- Fukuta S, Magnani JL, Twiddy EM, Holmes RK, Ginsburg V. 1988. Comparison of the carbohydrate-binding specificities of cholera toxin and *Escherichia coli* heat-labile enterotoxins Lth-I, LT-IIa, and LT-IIb. *Infect Immun* 56:1748–1753.
- Marketon MM, DePaolo RW, DeBord KL, Jabri B, Schneewind O. 2005. Plague bacteria target immune cells during infection. *Science* 309:1739–1741. <http://dx.doi.org/10.1126/science.1114580>.
- Zlokarnik G, Negulescu PA, Knapp TE, Mere L, Bures N, Feng L, Whitney M, Roemer K, Tsien RY. 1998. Quantitation of transcription and clonal selection of single living cells with beta-lactamase as reporter. *Science* 279:84–88. <http://dx.doi.org/10.1126/science.279.5347.84>.
- Blum FC, Przedpelski A, Tepp WH, Johnson EA, Barbieri JT. 2014. Entry of a recombinant, full-length, atoxic tetanus neurotoxin into Neuro-2a cells. *Infect Immun* 82:873–881. <http://dx.doi.org/10.1128/IAI.01539-13>.
- Lencer WI, Hirst TR, Holmes RK. 1999. Membrane traffic and the cellular uptake of cholera toxin. *Biochim Biophys Acta* 1450:177–190. [http://dx.doi.org/10.1016/S0167-4889\(99\)00070-1](http://dx.doi.org/10.1016/S0167-4889(99)00070-1).
- Donta ST, Beristain S, Tomicic TK. 1993. Inhibition of heat-labile cholera and *Escherichia coli* enterotoxins by brefeldin A. *Infect Immun* 61:3282–3286.
- Tremblay JM, Kuo CL, Abeijon C, Sepulveda J, Oyler G, Hu X, Jin MM, Shoemaker CB. 2010. Camelid single domain antibodies (VHHs) as neuronal cell intrabody binding agents and inhibitors of *Clostridium botulinum* neurotoxin (BoNT) proteases. *Toxicon* 56:990–998. <http://dx.doi.org/10.1016/j.toxicon.2010.07.003>.
- Liang S, Hosur KB, Lu S, Nawar HF, Weber BR, Tapping RI, Connell TD, Hajishengallis G. 2009. Mapping of a microbial protein domain involved in binding and activation of the TLR2/TLR1 heterodimer. *J Immunol* 182:2978–2985. <http://dx.doi.org/10.4049/jimmunol.0803737>.
- Van den Akker F, Sarfaty S, Twiddy EM, Connell TD, Holmes RK, Hol WG. 1996. Crystal structure of a new heat-labile enterotoxin, LT-IIb. *Structure* 4:665–678. [http://dx.doi.org/10.1016/S0969-2126\(96\)00073-1](http://dx.doi.org/10.1016/S0969-2126(96)00073-1).
- Whitemarsh RC, Tepp WH, Johnson EA, Pellett S. 2014. Persistence of botulinum neurotoxin subtypes 1–5 in primary rat spinal cord cells. *PLoS One* 9:e90252. <http://dx.doi.org/10.1371/journal.pone.0090252>.
- Mukherjee J, Tremblay JM, Leysath CE, Ofori K, Baldwin K, Feng X, Bedenice D, Webb RP, Wright PM, Smith LA, Tzipori S, Shoemaker CB. 2012. A novel strategy for development of recombinant antitoxin therapeutics tested in a mouse botulism model. *PLoS One* 7:e29941. <http://dx.doi.org/10.1371/journal.pone.0029941>.
- Dong J, Thompson AA, Fan Y, Lou J, Conrad F, Ho M, Pires-Alves M, Wilson BA, Stevens RC, Marks JD. 2010. A single-domain llama antibody potentially inhibits the enzymatic activity of botulinum neurotoxin by binding to the non-catalytic alpha-exosite binding region. *J Mol Biol* 397:1106–1118. <http://dx.doi.org/10.1016/j.jmb.2010.01.070>.

33. Zhang P, Ray R, Singh BR, Ray P. 2013. Mastoparan-7 rescues botulinum toxin-A poisoned neurons in a mouse spinal cord cell culture model. *Toxicon* 76:37–43. <http://dx.doi.org/10.1016/j.toxicon.2013.09.002>.
34. Zhang P, Ray R, Singh BR, Li D, Adler M, Ray P. 2009. An efficient drug delivery vehicle for botulism countermeasure. *BMC Pharmacol* 9:12. <http://dx.doi.org/10.1186/1471-2210-9-12>.
35. Edupuganti OP, Ovsepian SV, Wang J, Zurawski TH, Schmidt JJ, Smith L, Lawrence GW, Dolly JO. 2012. Targeted delivery into motor nerve terminals of inhibitors for SNARE-cleaving proteases via liposomes coupled to an atoxic botulinum neurotoxin. *FEBS J* 279:2555–2567. <http://dx.doi.org/10.1111/j.1742-4658.2012.08638.x>.
36. Jin R, Rummel A, Binz T, Brunger AT. 2006. Botulinum neurotoxin B recognizes its protein receptor with high affinity and specificity. *Nature* 444:1092–1095. <http://dx.doi.org/10.1038/nature05387>.
37. Chai Q, Arndt JW, Dong M, Tepp WH, Johnson EA, Chapman ER, Stevens RC. 2006. Structural basis of cell surface receptor recognition by botulinum neurotoxin B. *Nature* 444:1096–1100. <http://dx.doi.org/10.1038/nature05411>.
38. Dong M, Yeh F, Tepp WH, Dean C, Johnson EA, Janz R, Chapman ER. 2006. SV2 is the protein receptor for botulinum neurotoxin A. *Science* 312:592–596. <http://dx.doi.org/10.1126/science.1123654>.
39. Kuo CL, Oylar GA, Shoemaker CB. 2011. Accelerated neuronal cell recovery from botulinum neurotoxin intoxication by targeted ubiquitination. *PLoS One* 6:e20352. <http://dx.doi.org/10.1371/journal.pone.0020352>.
40. Mukherjee J, Dmitriev I, Debatis M, Tremblay JM, Beamer G, Kashentseva EA, Curiel DT, Shoemaker CB. 2014. Prolonged prophylactic protection from botulism with a single adenovirus treatment promoting serum expression of a VHH-based antitoxin protein. *PLoS One* 9:e106422. <http://dx.doi.org/10.1371/journal.pone.0106422>.
41. Lansbury PT, Lashuel HA. 2006. A century-old debate on protein aggregation and neurodegeneration enters the clinic. *Nature* 443:774–779. <http://dx.doi.org/10.1038/nature05290>.
42. Mueller NH, Gilden DH, Cohrs RJ, Mahalingam R, Nagel MA. 2008. Varicella zoster virus infection: clinical features, molecular pathogenesis of disease, and latency. *Neurol Clin* 26:675–697. <http://dx.doi.org/10.1016/j.ncl.2008.03.011>.
43. Blum FC, Chen C, Kroken AR, Barbieri JT. 2012. Tetanus toxin and botulinum toxin utilize unique mechanisms to enter neurons of the central nervous system. *Infect Immun* 80:1662–1669. <http://dx.doi.org/10.1128/IAI.00057-12>.
44. Prabakaran S, Tepp W, DasGupta BR. 2001. Botulinum neurotoxin types B and E: purification, limited proteolysis by endoproteinase Glu-C and pepsin, and comparison of their identified cleaved sites relative to the three-dimensional structure of type A neurotoxin. *Toxicon* 39:1515–1531. [http://dx.doi.org/10.1016/S0041-0101\(01\)00124-6](http://dx.doi.org/10.1016/S0041-0101(01)00124-6).
45. Malizio CJ, Goodnough MC, Johnson EA. 2000. Purification of Clostridium botulinum type A neurotoxin. *Methods Mol Biol* 145:27–39. <http://dx.doi.org/10.1385/1-59259-052-7:27>.